

Analytical Expression of Pulsating Torque Harmonics due to PWM Drives

Joseph Song-Manguelle, Gabriel Ekemb, Stefan Schröder,
Tobias Geyer, Jean-Maurice Nyobe-Yome, Rene Wamkeue

Abstract—This paper proposes an analytical approach to reconstruct the air gap torque waveform of an electrical motor from its stator voltages and currents. This approach is consistent with practical implementation requirements of large variable frequency drives, where a direct measurement of the air gap torque is generally not possible.

The method is based on an analytical reconstruction of the air gap torque in stationary and orthogonal coordinates. The proposed approach can be used as a design tool to accurately predict the frequencies of torque harmonics along with their magnitudes and phases. The results can be used to predict the shaft's torsional behavior and they can help assessing shear stresses of the shaft, thus providing a better understanding of the shaft's design life time. Moreover, the proposed approach is a tool for root cause analysis of drive failures. By reconstructing the air gap torque one can accurately prove whether or not one of the shaft's eigenmodes was excited.

The proposed technique is applied to a 35 MW drive system based on the parallel connection of four back-to-back neutral point clamped converters. Through simulations, the pulse-width modulated voltage source inverters are analyzed for different switching frequencies and over a wide operating range. The results confirm the accuracy of the proposed method.

Index Terms—Medium-voltage drive, megawatt drive, multi-level converter, liquefied natural gas, oil and gas, voltage source inverter, pulse width modulation, pulsating torque, torsional vibration.

I. INTRODUCTION

A rotating mechanical system is shown in Fig. 1. The shaft system is a combination of different energy storage elements such as inertia and stiffness constants. It has at least one natural frequency [1]. These eigenmodes can be excited, if an oscillatory external torque component is applied to the shaft system, with a frequency located at or near one of the shaft's natural frequencies. As a result, the magnitude of the corresponding shaft oscillation increases linearly with time—it is only limited by the damping elements of the system [1]. Depending on the torque magnitude and the duration of the stimulus torque, the shear stress on the shaft may be increased, leading to accelerated fatigue, life time reduction, and possibly eventually to system failure or shutdown.

Large rotating machines involving electric motors are subject to diverse disturbances. These disturbances can result in torque oscillations and may initiate twisting oscillations of the

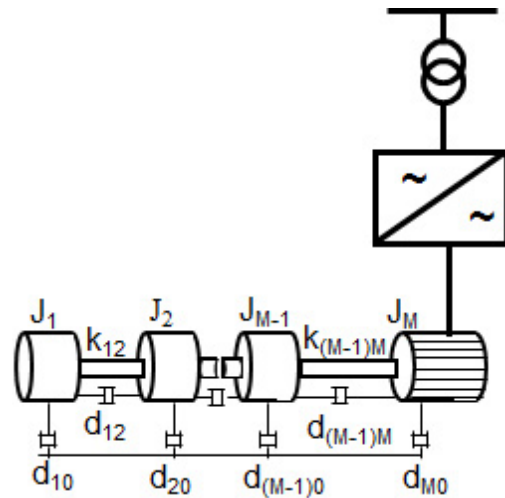


Fig. 1. General representation of a rotating shaft system with a VFD

rotating shaft. Among these disturbances, the motor's air gap torque components are one of the electromagnetic stimulus sources that can create such undesired phenomena. Electromagnetic stimulus forces are created by electromagnetic phenomena such as radial magnetic attraction between the stator, rotor and magneto-motive forces (MMFs) in the motor air gap [2]. These forces are influenced by the construction of the machine (slot construction in the stator or rotor, winding coefficients and air gap correction). MMFs are created by the voltage applied at the machine terminals.

For rotating shafts driven by variable speed drive systems, the voltage applied at the machine terminals is supplied by the variable frequency drive (VFD). VFDs create distorted voltages, which generate flux in the stator and produce current flows in the stator windings. It is the combination of flux and current that generates electromagnetic torque components in the motor's air gap.

Previous investigations have shown how to predict the frequencies of torque harmonics [4]–[6]. However, these relationships were not analytically demonstrated and torque magnitudes and phases were not calculated. This paper covers these limitations for pulse width modulated voltage source inverters and provides analytical expressions of the air gap torque components based on measured three-phase stator voltages and currents only. Simulations of a 35 MW PWM voltage source inverter (VSI) system confirm the accuracy of the results.

J. Song-Manguelle is with ExxonMobil Development, Houston, TX, USA, joseph.song@ieee.org

G. Ekemb is with the University of Chicoutimi, Chicoutimi, QC, Canada.

S. Schröder is with GE Global Research, Munich, Germany.

T. Geyer is with ABB Corporate Research, Baden-Dättwil, Switzerland.

J.M. Nyobe-Yome is with ENSET, the University of Douala, Cameroon.

Prof. R. Wamkeue is with the University of Quebec in Abitibi-Temiscamingue, Rouyn-Noranda, QC, Canada.

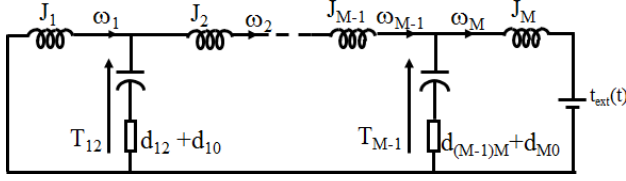


Fig. 2. Equivalent electrical circuit of a generalized shaft system

II. TORSIONAL RESONANCE EXCITATION DUE TO VFDS

A. Modeling and Excitation of the Rotating Shaft System

Previous investigations have shown that a rotating mechanical system as shown in Fig. 1 with multiple inertias J_1, \dots, J_M coupled by shaft elements with stiffness constants $k_{12}, \dots, k_{(M-1)M}$ and with damping coefficients $d_{12}, \dots, d_{(M-1)M}$ and d_{10}, \dots, d_{M0} behaves in a similar way as a multiple branch electrical circuit as shown in Fig. 2. From a phenomenological point of view, moments of inertia are equivalent to inductances, damping coefficients to resistances, and inverse stiffness constants to capacitances. Angular velocities can be seen as currents, and torques are equivalent to potential differences measured against a common reference [4]–[7].

In Fig. 2, J_M is the rotor inertia of the electric motor and t_{ext} is the set of electromagnetic torque components in the motor's air gap. These torque components are created by a combination of stator flux and current harmonics. The stator flux can be approximated as the time integral of the voltage applied to the stator windings. The stator voltages are supplied to the motor by the VFD. The switching inherent to power electronics introduces nonlinearities on the voltages generated by the VFD [3]. As a consequence, distorted voltage waveforms with non-fundamental frequency harmonics are fed to the stator windings. The voltage harmonics are not only converted to current harmonics through the machine impedance, but they also create a flux in the machine windings [5]. The combination of the stator flux harmonics and the current harmonics leads to torque harmonics in the motor's air gap¹. The motor air gap torque components are applied to the motor's rotor inertia as the externally applied torque t_{ext} .

If one of the external torque components has a frequency located at or near one of the shaft's natural frequencies, then the shaft's eigenmodes may be excited. This leads to an angular oscillation of the shaft with a magnitude linearly increasing with time. Consequently, this may lead to torque increases along the shaft resulting in accelerated fatigue and possibly in shaft-system failure. Fig. 3 summarizes the mechanism of the excitation of the shaft's natural frequencies. The shaft behaves in a similar way as an RLC circuit with multiple branches. The natural frequencies $f_{nat_0}, \dots, f_{nat_n}$ can be calculated as the roots of the characteristic equation of the circuit [8]. The air gap torque components generated by the motor are decomposed into a DC component T_{DC} and into multiple harmonics, which are applied to the inertia of the rotor. If at

¹It has been assumed that the machine is designed with winding coefficients to produce a sinusoidal magneto-motive force. Therefore, flux distortions due to the machine design are neglected.

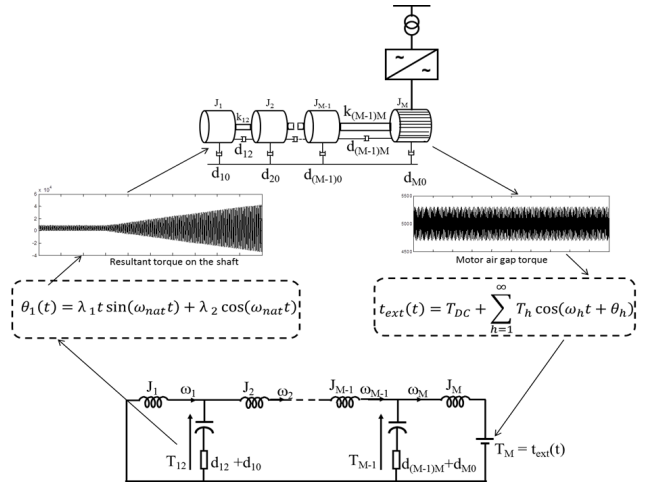


Fig. 3. Mechanism of the torsional excitation of a rotating shaft system by a VFD

least one of the torque harmonics has a frequency f_{te_n} located near one of the shaft natural frequencies,

$$[f_{nat_0}, \dots, f_{nat_n}] \approx [f_{te_1}, f_{te_2}, \dots, f_{te_m}] \quad (1)$$

the resulting torque along the shaft increases linearly with time [1].

B. Origin of the Motor Air Gap Torque Components

Regardless of the type of AC motor (synchronous or induction) used with the VFD, the torque developed in the motor's air gap is dependent on the applied voltage and the stator current. The relationship between the generated torque, the voltage and current is similar in both types of machines.

Consider the set of balanced three-phase voltages v_{abc} to be applied to the stator winding with different frequencies and magnitudes. The corresponding stator current is denoted by i_{sabc} . The motor's air gap torque is denoted by $t_e(t)$ when using SI quantities and is given by [5] as:

$$t_e(t) = \frac{3}{2} \frac{P}{2} (\psi_{s\alpha} i_{s\beta} - \psi_{s\beta} i_{s\alpha}), \quad (2)$$

where the factor $3/2$ stems from the peak invariant transformation and P denotes the number of poles. Adopting the stationary orthogonal coordinate system $\alpha\beta$, $\psi_{s\alpha}$ and $\psi_{s\beta}$ denote the stator flux components in the α and β -axis, respectively, and $i_{s\alpha}$ and $i_{s\beta}$ refer accordingly to the stator currents in $\alpha\beta$.

Consider an electrical quantity X_{abc} (such as a voltage, current, flux, etc.) in the three-phase system with the phases a , b and c . Using the Park transformation [5], the X_{abc} quantity can be transformed to the $\alpha\beta 0$ stationary reference frame according to

$$X_{\alpha\beta 0} = M X_{abc} \quad (3a)$$

$$M = \frac{2}{3} \begin{pmatrix} 1 & -1/2 & -1/2 \\ 0 & \sqrt{3}/2 & -\sqrt{3}/2 \\ 1/2 & 1/2 & 1/2 \end{pmatrix} \quad (3b)$$

For a balanced three-phase system, (3a) can be simplified to

$$X_\alpha = X_a \quad (4a)$$

$$X_\beta = (X_b - X_c)/\sqrt{3}. \quad (4b)$$

The flux ψ_s in (2) can be determined by taking into account the stator resistance R_s , the supplied voltage and the stator current. In the high power operating regime, the resistive losses of the stator can be neglected; the stator flux is then only dependent on the stator voltage:

$$\psi_{sabc} = \int (u_{sabc} - R_s i_{sabc}) dt \cong \int u_{sabc} dt. \quad (5)$$

Finally, the torque harmonic in (2) can be estimated based only on the voltage harmonics:

- The voltage harmonics applied to the stator windings are known based on the type of VFD and its control and/or modulation strategy. Therefore, the flux harmonics can be estimated.
- The stator current harmonics are located at the same frequencies as the voltage harmonics that created them, with their magnitude being dependent on the machine's total leakage impedance.

Neglecting the stator resistance simplifies the derivation. A more complete analysis can be done that includes the voltage drop due to the stator resistance. However, as simulation and tests results have shown for a 35 MW PWM VSI system [7], this assumption is valid for all operating points of this particular machine, because the stator flux due to the voltage drop on the stator resistance has a negligible magnitude, leading to a negligible error in the induced air gap torque components.

III. BASIC ANALYTICAL EXPRESSIONS OF THE TORQUE

A. Effect of Voltages Without Harmonics

Assume that the voltage applied to the stator is a symmetrical three-phase system without harmonics. The three-phase stator voltage and current sets can be written as

$$\begin{aligned} v_{sa} &= V_1 \cos(\omega t) & i_{sa} &= I_1 \cos(\omega t - \phi_1) \\ v_{sb} &= V_1 \cos\left(\omega t - \frac{2\pi}{3}\right) & i_{sb} &= I_1 \cos\left(\omega t - \frac{2\pi}{3} - \phi_1\right) \\ v_{sc} &= V_1 \cos\left(\omega t + \frac{2\pi}{3}\right) & i_{sc} &= I_1 \cos\left(\omega t + \frac{2\pi}{3} - \phi_1\right) \end{aligned} \quad (6)$$

Equivalently, in the orthogonal coordinate system, using the peak-invariant transformation, these quantities can be written as follows

$$\begin{aligned} v_{s\alpha} &= V_1 \cos(\omega t) & i_{s\alpha} &= I_1 \cos(\omega t - \phi_1) \\ v_{s\beta} &= V_1 \sin(\omega t) & i_{s\beta} &= I_1 \sin(\omega t - \phi_1) \end{aligned} \quad (7)$$

and the stator flux components are given by

$$\begin{aligned} \psi_{s\alpha} &\cong \int v_{s\alpha} dt = \frac{V_1}{\omega} \sin(\omega t) \\ \psi_{s\beta} &\cong \int v_{s\beta} dt = -\frac{V_1}{\omega} \cos(\omega t) \end{aligned} \quad (8)$$

Transforming the stator current and flux to the $\alpha\beta$ reference frame as shown in (7)–(8) and substituting them in the torque equation (2) yields

$$t_e = \frac{3}{2} \frac{P}{2} \frac{V_1 I_1}{\omega} \cos(\phi_1) \quad (9)$$

The result shows that if a symmetrical three-phase voltage system is applied to the stator windings, regardless of its frequency, a constant DC torque component (zero frequency) is created in the motor air gap. This DC torque component is the one that drives the motor.

B. Effect of Voltages with Negative Sequence Harmonics

Assume that the voltage applied to the stator windings is a symmetrical voltage with a fundamental component and one harmonic component located at five times the fundamental frequency:

$$\begin{aligned} v_{sa} &= V_1 \cos(\omega t) + V_5 \cos(5\omega t) \\ v_{sb} &= V_1 \cos\left(\omega t - \frac{2\pi}{3}\right) + V_5 \cos\left(5\omega t - 5\frac{2\pi}{3}\right) \\ v_{sc} &= V_1 \cos\left(\omega t + \frac{2\pi}{3}\right) + V_5 \cos\left(5\omega t + 5\frac{2\pi}{3}\right) \end{aligned} \quad (10)$$

Following a similar approach as in the previous subsection, the 5th harmonic component of the current has the phase angle ϕ_5 and the flux is taken approximately as the time integral of the voltage. Using the Park transformation to transform the stator voltages and currents from the abc system to the $\alpha\beta$ reference frame, computing the stator flux similar to (8) and inserting the results into the torque equation (2) results in the following air gap torque:

$$t_e(t) = T_{DC} + T_{6Neg} \cos(6\omega t + \phi_5) \quad (11a)$$

$$T_{DC} = \frac{3}{2} \frac{P}{2} \left(\frac{V_1 I_1}{\omega} \cos(\phi_1) - \frac{V_5 I_5}{5\omega} \cos(\phi_5) \right) \quad (11b)$$

$$T_{6Neg} = \frac{3}{2} \frac{P}{2} \left(\frac{V_1 I_5}{\omega} - \frac{V_5 I_1}{5\omega} \right) \quad (11c)$$

The resulting torque is composed of two components:

- An DC component, which is solely created by the interaction of voltages and currents located at the same frequency with their respective phases. The DC component represents the active power absorbed by the machine.
- A 6th harmonic component created by the interaction of the fundamental component of the voltage and the 5th harmonic component of the current, as well as the fundamental component of the current and the 5th harmonic component of the voltage.

C. Effect of Voltages with Positive Sequence Harmonics

Following a similar approach as in the previous subsection, it is assumed that the voltage applied at the stator windings is a symmetrical voltage with a fundamental component and a harmonic component located at seven times the fundamental, creating the 7th harmonic component of the current with the phase angle ϕ_7 . As previously, the resulting torque consists of two components, as shown in (12):

- An DC component, which is solely created by the interaction of voltages and currents located at the same frequency with their respective phases.
- A 6th harmonic component created by the interaction of the fundamental component of the voltage and the 7th harmonic component of the current, as well as the fundamental component of the current and the 7th harmonic component of the voltage.

$$t_e(t) = T_{DC} + T_{6Pos} \cos(6\omega t + \phi_7) \quad (12a)$$

$$T_{DC} = \frac{3P}{2} \left(\frac{V_1 I_1}{\omega} \cos(\phi_1) + \frac{V_7 I_7}{7\omega} \cos(\phi_7) \right) \quad (12b)$$

$$T_{6Pos} = \frac{3P}{2} \left(\frac{V_1 I_7}{\omega} + \frac{V_7 I_1}{7\omega} \right) \quad (12c)$$

D. A Generic Formulation of the Basic Campbell Diagram

1) *Preliminary Considerations:* It is beneficial to understand the phase sequences of the harmonics in electrical systems and how they behave in the stationary reference frame. This will allow us to provide insight into the way torque harmonics are created and to easily correlate the location of voltage and current harmonics and their corresponding torque harmonic components in the frequency domain. The rank of all harmonics can be represented in a generic form as

$$\begin{aligned} n_{pos} &= 6l + 1 \\ n_{neg} &= 6l - 1 \\ n_{zero} &= 3l \\ \forall l &= 0, 1, 2, 3, \dots \end{aligned} \quad (13)$$

where n_{pos} , n_{neg} and n_{zero} respectively represent the rank of positive, negative and zero sequence harmonic components with respect to the fundamental $n = 1$. Harmonic ranks including the fundamental can be written in compact form as

$$n \in \{n_{zero}, n_{neg}, n_{pos}\}. \quad (14)$$

It may be beneficial to note that:

- All zero sequence harmonics such as the 3rd harmonic and all integer multiple of 3 (i.e. 6th, 9th, 12th, etc.) are all in phase with each other, regardless of the fact that their respective fundamentals are 120 degrees out of phase. Their phase is not affected by the transformation into stationary coordinates.
- All positive sequence harmonics such as the 7th, 13th, 19th and so on are rotating in the same direction as the fundamental component in stationary coordinates. They both have non-zero α and β -components and their overall vector rotation is in the same direction as the fundamental when they are transformed into stationary coordinates.
- All negative sequence harmonics such as the 5th, 11th, 17th and so on are rotating in the opposite direction of the fundamental component in stationary coordinates. When they are transformed into stationary coordinates, they both have non-zero α and β -components, with the β -component having a negative sign, and the overall vector rotation being in the opposite direction of the fundamental.

2) *Formulation of the Campbell Diagram:* Based on (11) and (12), the following statements can be formulated:

- The air gap torque created by a symmetrical three-phase system with a $(n_{neg})^{th}$ negative sequence harmonic has a DC component with a magnitude dependent on the phase angle of that negative sequence component, and a harmonic torque pulsating at $(n_{neg} + 1)$ times the fundamental frequency.
- The air gap torque created by a symmetrical three-phase system with a $(n_{pos})^{th}$ positive sequence harmonic has a

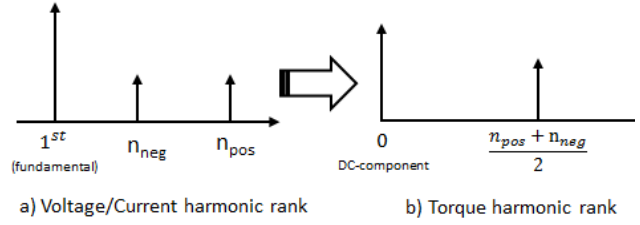


Fig. 4. Transformation of electrical negative and positive sequence harmonics to an air gap torque harmonic

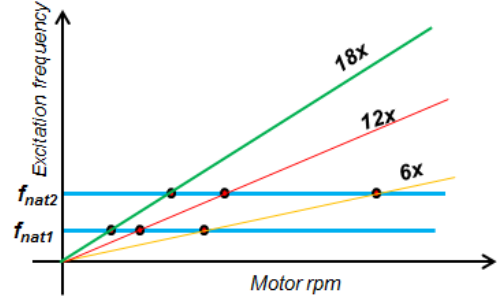


Fig. 5. Basic Campbell diagram of the air gap torque due to a VFD

- DC component with a magnitude dependent on the phase angle of that positive component, and a harmonic torque pulsating at $(n_{pos} - 1)$ times the fundamental frequency.
- A positive voltage harmonic component n_{pos} and a negative harmonic component n_{neg} create a torque harmonic component of order $n_{t_e} = 0.5(n_{neg} + n_{pos})$.

Therefore, the 5th and 7th voltage or current harmonics create a torque harmonic at 6 times the fundamental frequency. Similarly, the 11th and 13th create a torque harmonic at the 12th, the 17th and 19th create a torque harmonic at the 18th, and so on. Fig. 4 summarizes these results and Fig. 5 shows a basic Campbell diagram of the air gap torque due to a VFD. In this figure, f_{nat1} and f_{nat2} correspond to two natural frequencies of a given shaft. The solution of (1) is illustrated as red dots in the figure and corresponds to intersections between air gap torque frequencies and natural frequencies of the shaft. In the vicinity of those operating points the rotating shaft may be excited by the VFD.

IV. ANALYTICAL EXPRESSIONS OF THE AIR GAP TORQUE HARMONICS DUE TO PWM VSIS

A. Preliminary Considerations

Voltage spectra of pulse-width-modulated VSI were analytically calculated by Holmes, McGrath and Lipo [9]–[10]. Using the double Fourier transformation, the authors have analytically calculated the voltage spectrum of different PWM strategies, such as naturally sampled, regularly sampled, third harmonic reference injection (which is similar to space-vector modulation), discontinuous PWM, etc. for a wide range of VSI topologies, such as two-level, three-level and multi-level topologies, including the neutral point clamped (NPC) topology and series connected H-bridges. The results show that the voltage harmonic spectrum of a VSI is clearly dependent

on the selected topology as well as on the type of PWM used to modulate the VFD.

The importance of the aforementioned authors' results for drive-motor-load integration is emphasized in this section. The voltage harmonic spectrum of PWM VSI is characterized by the carrier frequency f_c , the fundamental frequency f_0 and their integer multiples m and n , with m referring to the integer multiples of the carrier frequency and n to multiples of the fundamental frequency. Each voltage harmonic h_{mn} can be written as

$$h_{mn}(t) = C_{mn} \cos(m(\omega_c t + \theta_c) + n(\omega_0 t + \theta_0) + \theta_{mn}), \quad (15)$$

where $\omega_c = 2\pi f_c$ and $\omega_0 = 2\pi f_0$; θ_c and θ_0 are respectively the phases of the carrier and the fundamental; C_{mn} and θ_{mn} are expressions dependent on the modulation scheme.

For PWM VSI, the following statements can be made.

i) Even values of m are paired with odd values of n :

$$\begin{aligned} m &= 2i, \forall i = 0, 1, 2, 3, \dots \\ n &= 2j + 1, \forall j = 0, \pm 1, \pm 2, \pm 3, \dots \end{aligned} \quad (16)$$

In (16) j should be chosen such that all triplen harmonics are excluded. If n is an integer multiple of 3, the corresponding harmonic is of zero sequence. Since no zero sequence current can flow into a three-phase machine (whose star point is not connected), these harmonics can be excluded. Therefore, the positive and negative sequence harmonics can be written as

$$\begin{aligned} n_{pos} &= 6l + 1, \forall l = 0, \pm 1, \pm 2, \pm 3, \dots \\ n_{neg} &= 6l - 1. \end{aligned} \quad (17)$$

ii) Odd values of m are paired with even values of n , i.e.

$$\begin{aligned} m &= 2i + 1, \forall i = 0, 1, 2, 3, \dots \\ n &= 2j, \forall j = 0, \pm 1, \pm 2, \pm 3, \dots \end{aligned} \quad (18)$$

In this case, the positive and negative sequence harmonics can be written as follows:

$$\begin{aligned} n_{pos} &= 6l - 2, \forall l = 0, \pm 1, \pm 2, \pm 3, \dots \\ n_{neg} &= 6l + 2. \end{aligned} \quad (19)$$

iii) All other combinations yield zero amplitudes of the corresponding harmonic.

It is important to note that the definition of the harmonic sequences is mainly linked to the phase-shift θ_0 of the fundamental component. Therefore the analytical development of the torque (2) can be adapted based on the previous approach, and the torque harmonic frequencies can be extracted by following the same principle. Phase sequences are then defined according to harmonic positions with respect to f_0 , i.e. with the value of n . The torque can be expressed as a product of the stator flux and stator currents in orthogonal coordinates.

B. General Formulation

Assume that a voltage harmonic is given by (20), and a current harmonic is given by (21):

$$v_{m_v n_v}(t) = V_{m_v n_v} \cos(m_v \omega_c t + n_v \omega_0 t + \theta_{m_v n_v}) \quad (20)$$

$$i_{m_i n_i}(t) = I_{m_i n_i} \cos(m_i \omega_c t + n_i \omega_0 t + \theta_{m_i n_i}) \quad (21)$$

The parameters m_v , n_v and m_i , n_i are integer constants. Following the principle described in the previous subsections, the harmonic stator current and flux in the $\alpha\beta$ reference frame can be written as follows:

$$i_{s\alpha m_i n_i} = I_{m_i n_i} \cos(m_i \omega_c t + n_i \omega_0 t + \theta_{m_i n_i}) \quad (22a)$$

$$i_{s\beta m_i n_i} = \varepsilon_i I_{m_i n_i} \sin(m_i \omega_c t + n_i \omega_0 t + \theta_{m_i n_i}) \quad (22b)$$

$$\psi_{s\alpha m_v n_v} = \Psi_{m_v n_v} \sin(m_v \omega_c t + n_v \omega_0 t + \theta_{m_v n_v}) \quad (22c)$$

$$\psi_{s\beta m_v n_v} = -\varepsilon_v \Psi_{m_v n_v} \cos(m_v \omega_c t + n_v \omega_0 t + \theta_{m_v n_v}), \quad (22d)$$

where the flux magnitude $\Psi_{m_v n_v}$ is given by

$$\Psi_{m_v n_v} = \frac{V_{m_v n_v}}{m_v \omega_c + n_v \omega_0} \quad (23)$$

and the coefficients ε_{n_v} and ε_{n_i} are $\in (-1, 1)$. Triplen harmonics are not considered, i.e. for $n_v, n_i \neq 0, 3, 6, 9, \dots$

$$\varepsilon_{n_v} = \frac{2}{\sqrt{3}} \sin\left(n_v \frac{2\pi}{3}\right), \quad \varepsilon_{n_i} = \frac{2}{\sqrt{3}} \sin\left(n_i \frac{2\pi}{3}\right). \quad (24)$$

The interaction between the flux harmonic (created by the voltage harmonic $v_{m_v n_v}(t)$) and the current harmonic $i_{m_i n_i}(t)$ produces the torque harmonic

$$t_{eh}(t) = T_{eh} \cos(\omega_h t + \theta_h) \quad (25)$$

with the magnitude, frequency and phase given by

$$T_{eh} = \varepsilon_{n_v} \frac{3P}{2} \frac{V_{m_v n_v}}{m_v \omega_c + n_v \omega_0} I_{m_i n_i} \quad (26a)$$

$$\omega_h = \left(m_i - \frac{\varepsilon_{n_i} m_v}{\varepsilon_{n_v}}\right) \omega_c + \left(n_i - \frac{\varepsilon_{n_i} n_v}{\varepsilon_{n_v}}\right) \omega_0 \quad (26b)$$

$$\theta_h = \theta_{m_i n_i} - \frac{\varepsilon_{n_i}}{\varepsilon_{n_v}} \theta_{m_v n_v}. \quad (26c)$$

The relationships given in (25) and (26) correspond to the harmonic components of the air gap torque in induction and synchronous motors, when supplied by a voltage with harmonics, such as in variable speed drive applications. Depending on the inverter, the carrier frequency ω_c needs to be adapted, as well as the specific values of the parameters m_v, n_v, m_i and n_i . These relationships can also be extended to asynchronous and synchronous generators, where the voltage corresponds to the voltage generated by the machine. Using the notion of superposition, they can be used as the external torque t_{ext} in the electromechanical model of the rotating shaft shown in Fig. 2.

C. Relevant Torque Harmonics in PWM VSIs

Based on the previous relationships, the following statements can now be formulated:

i) In PWM drives $\omega_c \gg \omega_0$ usually holds. Then, according to (26a), the torque harmonic has a small magnitude T_{eh} if $m_v \neq 0$. In fact, this harmonic is of a relevant magnitude only when it is due to voltage baseband frequencies, i.e. when $m_v = 0$.

²For load-commutated inverters, ω_c represents the grid frequency and m_v, m_i, n_v and n_i are defined according to the pulse numbers for the grid and the motor side, respectively [6].

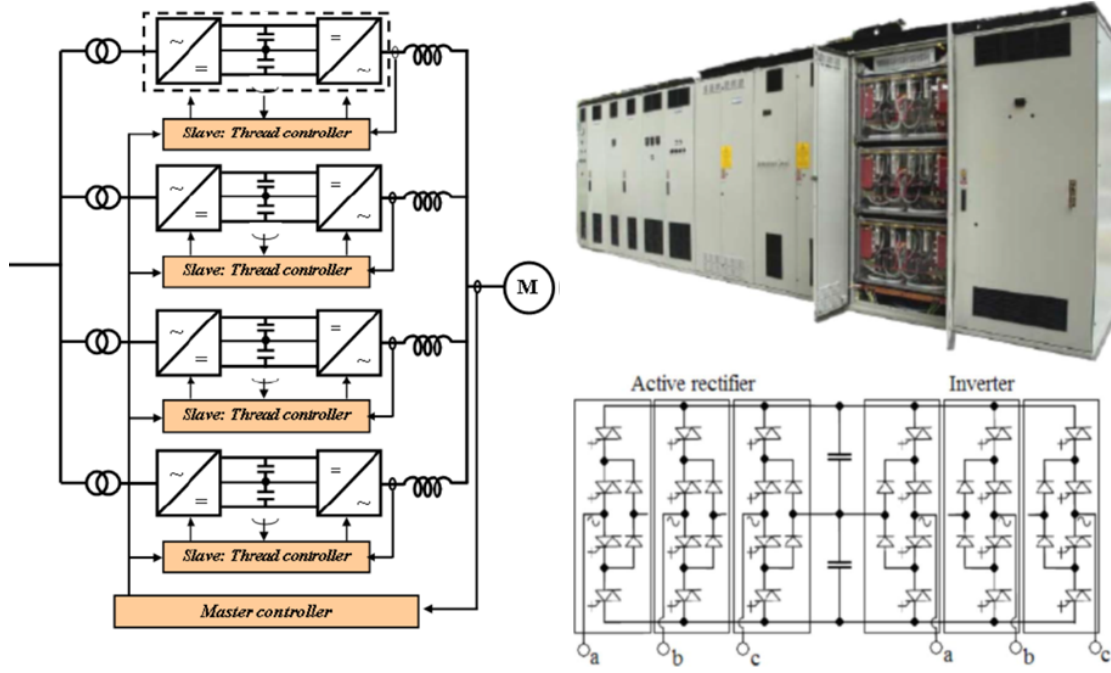


Fig. 6. Simplified representation of the 35 MW validation system

- ii) The magnitude T_{eh} is larger when the voltage or current harmonic is a fundamental component, because V_{01} and I_{01} are always the largest components compared to other harmonics.
- iii) All other combinations yield negligible torque magnitudes in the motor's air gap.

1) *A Note on the DC Torque Component:* Eq. (26) shows that only interactions between a current harmonic and a flux harmonic (created by a voltage harmonic) located at the same frequency as the current harmonic generate a DC torque component:

$$m_i = \frac{\varepsilon_{n_i} m_v}{\varepsilon_{n_v}}, \quad n_i = \frac{\varepsilon_{n_i} n_v}{\varepsilon_{n_v}}. \quad (27)$$

According to item (i) above, a torque with significant magnitude will be generated for $m_v = 0$, i.e. $m_i = 0$. Therefore, a DC torque component T_{DC} will be generated only when there is an interaction between a current and a flux harmonic located at the same frequency, i.e. $n_v = n_i = n$. The notation of the current and voltage harmonics can be simplified as $I_{0n} = I_n$ and $V_{0n} = V_n$, and T_{DC} can be written as

$$T_{DC} = \frac{2}{\sqrt{3}} \sin\left(n \frac{2\pi}{3}\right) \frac{3P}{2} \frac{V_n I_n}{2n\omega_0} \cos(\theta_{vn} - \theta_{iv}), \quad (28)$$

where θ_{vn} and θ_{iv} correspond to the phase angle of the voltage and current harmonic, respectively.

2) *Effects of Voltage Harmonics:* According to (26), the magnitude of torque components has a relevant value only for $m_v = 0$. That means only baseband harmonics of the voltage will remain and will mainly interact with the fundamental component of the current.

In (26), the parameters are set to $m_v = 0$, $m_i = 0$ and $n_i = 1$, leading to the frequency of the torque harmonic

$$\omega_h = (1 - \varepsilon_{n_v} n_v) \omega_0. \quad (29)$$

Note that n_v can be a negative or a positive sequence component with respect to the fundamental:

$$\begin{aligned} n_{v,neg} = 6l - 1 &\Rightarrow T_{eh} = -\frac{3P}{2} \frac{V_{6l-1}}{2(6l-1)\omega_0} I_1 \\ n_{v,pos} = 6l + 1 &\Rightarrow T_{eh} = \frac{3P}{2} \frac{V_{6l+1}}{2(6l+1)\omega_0} I_1 \end{aligned} \quad (30)$$

$$\omega_h = (6l) \omega_0 \quad \forall l = 0, \pm 1, \pm 2, \pm 3 \dots$$

This result explains why baseband harmonics at multiples of six times the fundamental frequency are present in the Campbell diagram of a machine supplied by a PWM VSI [7].

3) *Effects of Current Harmonics:* According to (26) and following the derivations in the previous subsection, current harmonics generate torque harmonics with relevant magnitudes when they interact with the fundamental component of the voltage. This corresponds to $m_v = 0$ and $n_v = 1$ (implying $\varepsilon_{n_v} = 1$) and arbitrary m_i and n_i . Omitting the phase, (26) becomes:

$$T_{eh} = \frac{3P}{2} \frac{V_1}{2\omega_0} I_{m_i n_i} \quad (31a)$$

$$\omega_h = m_i \omega_c + (n_i - \varepsilon_{n_i}) \omega_0 \quad (31b)$$

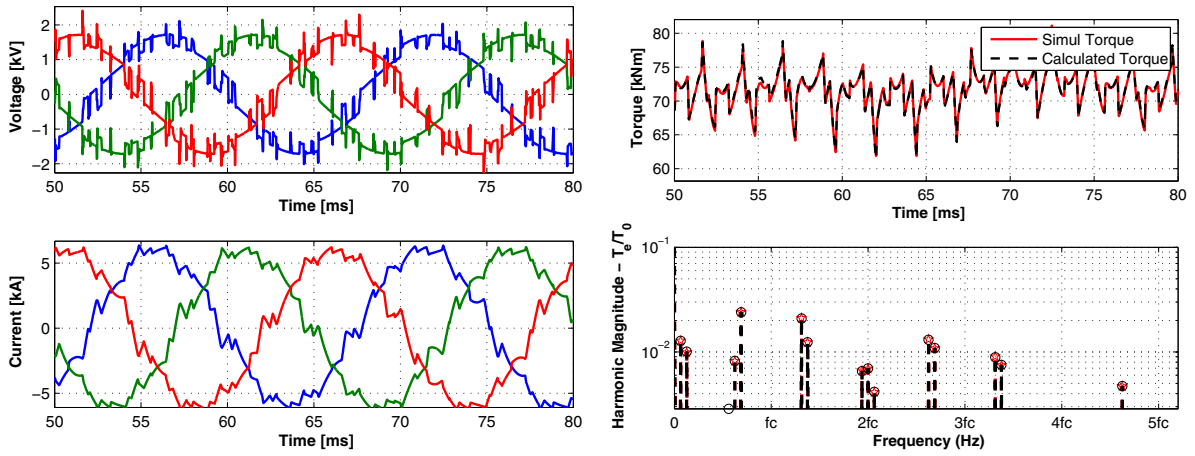
- For sidebands around even multiples of the carrier frequency, m_i and n_i are given according to (17). Taking into account the fundamental, negative and positive sequence components yields:

$$T_{eh,neg} = \frac{3P}{2} \frac{V_1}{2\omega_0} I_{2i,6l-1} \quad (32)$$

$$\omega_{h,neg} = 2i\omega_c + 6l\omega_0$$

$$T_{eh,pos} = \frac{3P}{2} \frac{V_1}{2\omega_0} I_{2i,6l+1} \quad (33)$$

$$\omega_{h,pos} = 2i\omega_c + 6l\omega_0$$



(a) Three-phase stator voltages and currents

(b) Simulated and reconstructed torque in the time and frequency domains

Fig. 7. Simulation results for the carrier frequency $f_c = 625$ Hz and the fundamental frequency $f_0 = 65$ Hz

- For sidebands around odd multiples of the carrier frequency, m_i and n_i are given according to (19). Taking into account negative and positive sequence components yields:

$$\begin{aligned} T_{eh,neg} &= \frac{3}{2} \frac{P}{\omega_0} V_1 I_{2i+1,6l+2} \\ \omega_{h,neg} &= (2i+1)\omega_c + [(6l+2)+1]\omega_0 \\ &= (2i+1)\omega_c + 3(2l+1)\omega_0 \end{aligned} \quad (34)$$

$$\begin{aligned} T_{eh,pos} &= \frac{3}{2} \frac{P}{\omega_0} V_1 I_{2i+1,6l-2} \\ \omega_{h,pos} &= (2i+1)\omega_c + [(6l-2)-1]\omega_0 \\ &= (2i+1)\omega_c + 3(2l-1)\omega_0 \end{aligned} \quad (35)$$

The relationships provided in (30)–(35) justify the location of torque harmonic frequencies as given in [7] and complement the torque expressions with their magnitudes. For a given current or voltage harmonic, the positive and negative sequence harmonics generate a torque component at the same frequency. The phases of the torque components are given in (26c).

V. VALIDATION

A. Principle of Validation

A compressor test bed rated at 35 MW and based on a parallel connection of PWM VSI systems with four back-to-back three-level neutral point clamped (NPC) inverters was used for validation purposes. The overall system is shown in Fig. 6. The validation procedure included computer simulations in Saber and Matlab, a scaled-down drive system as software evaluation platform and a full-scale system test facility. The design procedure and its detailed implementation were provided in [17]. Experimental test results as well as other design aspects of the system were discussed in [4]. Using Saber, selected simulation results that correlate current and voltage harmonics with torque harmonics in the frequency domain were presented in [7].

For the specific validation of the analytical expressions of the torque harmonics presented in this paper, post-processed results of simulations of the full-scale system are discussed

in this section. The results show a good correlation between calculations and simulations.

B. Simulation Results

Selected post-processed results are shown in Figs. 7 and 8 for a fundamental frequency of 65 Hz and 100 Hz, respectively. The carrier frequency was set to $f_c = 625$ Hz. In these simulations, the PWM signals of all four converters were synchronized and the system behaves like a single NPC drive. The voltages applied to the machine windings are shown in Fig. 7(a) and Fig. 8(a) along with the stator currents. The simulated torque is shown in Fig. 7(b) and Fig. 8(b), both in the time domain and in the frequency domain. In the time domain, the red straight line is the motor's air gap torque magnitude resulting from SABER simulations, and the black dashed line corresponds to the torque magnitude reconstructed based on the analytical expressions provided in this paper. In the frequency domain, the red star markers show simulated magnitude of the motor air gap torque components resulting from SABER simulations and the black dashed line shows the calculated results.

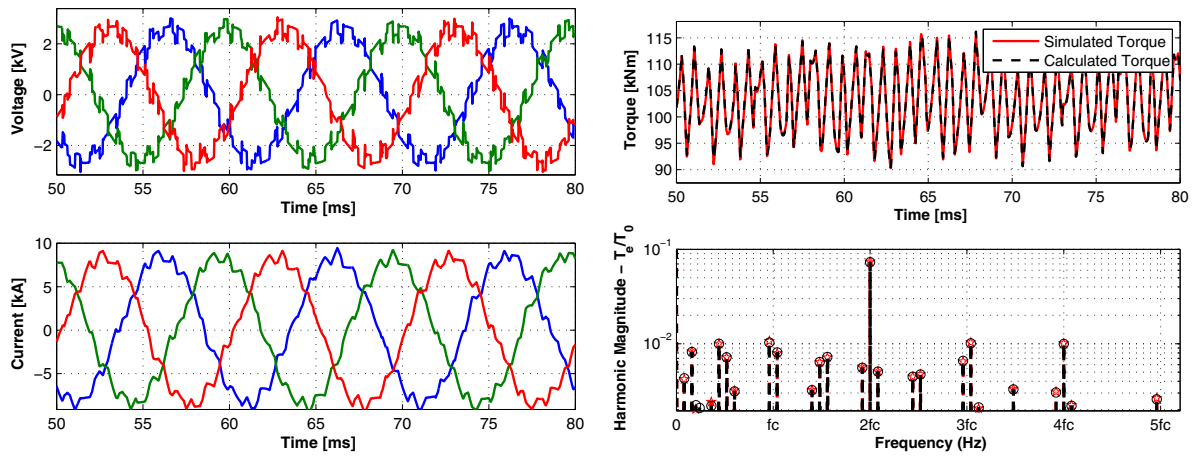
The results show a good accuracy between the simulated and the calculated torque.

VI. CONCLUSION

An analytical approach to reconstruct the air gap torque waveform of an electrical motor from its stator voltages and currents was proposed in this paper. The reconstruction is done in the stationary and orthogonal coordinates for simplification purposes. A generic air gap torque harmonic expression resulting from the interaction between a given current harmonic and a flux harmonic (created by voltage harmonic) has been derived. The result has been extended to a motor supplied by a PWM VSI.

Analytical results have shown that:

- A DC torque component is generated only when there is an interaction between a current and a flux harmonic located at the same frequency;



(a) Three-phase stator voltages and currents

(b) Simulated and reconstructed torque in the time and frequency domains

Fig. 8. Simulation results for the carrier frequency $f_c = 625$ Hz and the fundamental frequency $f_0 = 100$ Hz

- ii) Baseband torque harmonics multiple of six times the fundamental frequency are created due to the interaction between voltage baseband harmonics and the fundamental component of the current. Therefore, positive and negative sequence voltage harmonics create the same torque component.
- iii) Sideband torque harmonics are created due to the interaction between sideband current harmonics and the fundamental component of the voltage.

The proposed analytical expressions can be used for a better prediction of fatigue life of rotating machinery [11] or, as a tool to improve practical design against torsional vibrations [12]-[15]. Finally, they can also be extended to LCIs [16], with appropriate parameters (m_v, n_v) and (m_i, n_i) , depending on the number of pulses on the rectifier or on the inverter sides. Specifically for LCIs, motor's air gap torque components are mainly created due to the interaction between current harmonics resulting from the LCI and the flux created by the fundamental component of the back electromotive force of a synchronous motor.

REFERENCES

- [1] J. Song-Manguelle, C. Sihler, J. M. Nyobe-Yome, *Modeling of torsional resonances for multi-megawatt drives design*, IEEE IAS 43rd Annual Meeting, Oct. 2008, Edmonton, Canada.
- [2] D. Walker, *Torsional vibration of turbomachinery*, McGraw-Hill, 2004.
- [3] B. Wu, *High-power converters and AC drives*, IEEE Press, 2006.
- [4] S. Schröder, P. Tenca, T. Geyer, P. Soldi, L. Garces, R. Zhang, T. Toma and P. Bordignon, *Modular high-power shunt-interleaved drive system: A realization up to 35 MW for oil & gas applications*, IEEE Trans. on Industry Appl., vol. 46, no. 2, pp. 821-830, Mar./Apr. 2010.
- [5] P. C. Krause, O. Wasynczuk, S. D. Sudhoff, *Analysis of Electric Machinery and Drive Systems*, 2nd. ed., IEEE Press, Wiley Interscience, 2002.
- [6] J. Song-Manguelle, J. M. Nyobe-Yome, G. Ekemb, *Pulsating Torques in PWM Multi-megawatt Drives for Torsional Analysis of Large Shafts*, IEEE Trans. on Industry Appl., vol. 46, no. 1, pp. 130-138, Jan./Feb. 2010.
- [7] J. Song-Manguelle, S. Schröder, T. Geyer, G. Ekemb, J. M. Nyobe-Yome, *Prediction of Mechanical Shaft Failures due to Variable Frequency Drives*, IEEE Trans. on Industry Appl., vol. 25, no. 4, pp. 130-138, Jan./Feb. 2010.
- [8] C. Mung-Ong, *Dynamic Simulation of Electric Machinery using Matlab/Simulink*, Prentice Hall, Purdue, 1999.
- [9] D. G. Holmes, B. P. McGrath, *Opportunities for Harmonic Cancellation with Carrier-based PWM for Two-Level and Multilevel Cascaded Inverters*, IEEE Trans. on Industry Appl., vol. 37, no. 2, pp. 574-582, Mar./Apr. 2001.
- [10] D. G. Holmes, T. A. Lipo, *Pulse Width Modulation for Power Converters: Principle and Practice*, IEEE Press, Series on Power Eng., Wiley Interscience, 2003.
- [11] Xu Han, A. B. Palazzolo *VFD Machinery Vibration Fatigue Life and Multi-level Inverter Effect*, IEEE IAS 47rd Annual Meeting, Oct. 2012, Las Vegas, NV, USA.
- [12] M. A. Corbo, S. B. Malanoski *Practical Design against Torsional Vibration*, Proceedings of the 25th Turbomachinery Symposium, Turbomachinery Laboratory, Texas A&M University, College Station, Texas, pp. 189-222, 1996.
- [13] T. F. Kaiser, R. H. Osman, R. O. Dickau *Analysis Guide for Variable Frequency Drive Operated Centrifugal Pump*, Proceedings of the 24th International pump Users Symposium, Texas A&M University, College Station, Texas, pp. 81-106, 2008.
- [14] J. A. Kocur, J. Corcoran *VFD Induced Coupling Failure*, Case Study no. 9, The 37th Turbomachinery Symposium, Texas A&M University, College Station, Texas, 2008.
- [15] H. McArthur, M. Falk, M. Bertel, *VFD Induced Coupling Torque Pulsations: Cause of Mine Exhaust Fan Coupling failures*, The 14th U.S./North American Mine Ventilation Symposium Salt Lake City, Utah, 2012.
- [16] V. Hütten, R. M. Zurowski, M. Hilsher, *Torsional Interharmonic Interaction Study of 75 MW Direct-Driven VSDS Motor Compressor Trains for LNG Duty*, Proceedings of the 37th Turbomachinery Symposium, Turbomachinery Laboratory, Texas A&M University, College Station, Texas, pp. 57-66, 2008.
- [17] R. Baccani, R. Zhang, et al., *Electric System for High Power Compressor Trains in Oil and Gas Applications - System Design, Validation Approach and Performance*, Proc. 36th Turbomach. Symp., Texas A&M Univ., College Station, TX, 2007.